Published in final edited form as:
Science. 2010 July 23; 329(5990): 454–457. doi:10.1126/science.1188280.

Sfrp5 Is an Anti-Inflammatory Adipokine That Modulates Metabolic Dysfunction in Obesity

Noriyuki Ouchi[1,*], **Akiko Higuchi**[1], **Koji Ohashi**[1], **Yuichi Oshima**[1], **Noyan Gokce**[2], **Rei Shibata**[3], **Yuichi Akasaki**[1], **Akihiko Shimono**[4], and **Kenneth Walsh**[1,*]

[1]Molecular Cardiology and Whitaker Cardiovascular Institute, Boston University School of Medicine, 715 Albany Street, W611, Boston, MA 02118, USA.

[2]Evans Department of Medicine and Whitaker Cardiovascular Institute, Boston University School of Medicine, 715 Albany Street, E703E, Boston, MA 02118, USA.

[3]Department of Cardiology, Nagoya University Graduate School of Medicine, Showa-ku, Nagoya 466-8550, Japan.

[4]Cancer Science Institute of Singapore, National University of Singapore, Centre of Life Sciences, 28 Medical Drive, no. 02-07, Singapore 117456.

Abstract

Adipose tissue secretes proteins referred to as adipokines, many of which promote inflammation and disrupt glucose homeostasis. Here we show that secreted frizzled-related protein 5 (Sfrp5), a protein previously linked to the Wnt signaling pathway, is an anti-inflammatory adipokine whose expression is perturbed in models of obesity and type 2 diabetes. Sfrp5-deficient mice fed a high-calorie diet developed severe glucose intolerance and hepatic steatosis, and their adipose tissue showed an accumulation of activated macrophages that was associated with activation of the c-Jun N-terminal kinase signaling pathway. Adenovirus-mediated delivery of Sfrp5 to mouse models of obesity ameliorated glucose intolerance and hepatic steatosis. Thus, in the setting of obesity, Sfrp5 secretion by adipocytes exerts salutary effects on metabolic dysfunction by controlling inflammatory cells within adipose tissue.

Obesity is a predisposing factor for metabolic disorders, such as type 2 diabetes, which are often associated with a low-grade inflammatory state in adipose tissue. Adi-pose tissue secretes a variety of cytokines, referred to as adipokines (*1–3*). Most adipokines—such as tumor necrosis factor a (TNFa), interleukin-6 (IL-6), and leptin—are proinflammatory. One prominent exception is adiponectin (APN), an anti-inflammatory adipokine that promotes insulin sensitization and protects cardiovascular tissue from ischemic injury (*2, 4*).

Because adipokine dysregulation can contribute to the pathogenesis of obesity-linked disorders, we sought to identify new adipokines by comparing the gene expression profile of adipose tissue from lean mice with that from obese mice fed a high-fat, high-sucrose (HF-HS) diet (*5, 6*). Of numerous candidates, we found that secreted frizzled-related protein (Sfrp) 5 was expressed at substantially higher levels in white adipose tissue than in other

[*]To whom correspondence should be addressed: kxwalsh@bu.edu (K.W.); nouchi@bu.edu (N.O.).

Supporting Online Material
www.sciencemag.org/cgi/content/full/science.1188280/DC1
Materials and Methods
Figs. S1 to S11
References

tissues at both the transcript and protein levels and that the Sfrp5 transcript was confined to adipocytes rather than stromal vascular cells (fig. S1). Sfrp proteins sequester Wnt proteins in the extracellular space and prevent Wnt binding to their receptors (*7, 8*). Canonical Wnt signaling negatively regulates adipogenesis (*9*), but little is known about the role of Sfrp5 in the control of noncanonical Wnt signaling in adipose tissue or in the regulation of systemic metabolism.

To investigate Sfrp5 regulation during metabolic dysfunction, we examined its expression in rodent models of obesity (*6*). Sfrp5 expression was reduced in obese leptin-deficient (ob/ob) mice (Fig. 1A) and Zucker diabetic fatty rats (fig. S2). Sfrp5 expression was also reduced in wild-type (WT) mice fed a HF-HS diet for 24 weeks (Fig. 1B), but Sfrp5 expression was transiently up-regulated after 12 weeks of the diet, when metabolic dysfunction and adipose tissue expression of markers of inflammation, macrophage infiltration, and oxidative and endoplasmic reticulum stresses are less severe (fig. S3). Sfrp5 has been shown to bind and antagonize both Wnt5a and Wnt11 (*10*). Wnt5a protein expression, but not Wnt11, could be detected in adipose tissues (Fig. 1 and figs. S2 and S3). In all models examined, obesity led to higher levels of Wnt5a expression and an increase in the ratio of Wnt5a to Sfrp5.

To determine whether Sfrp5 regulation is relevant to human obesity, we analyzed visceral fat biopsy specimens of obese individuals. Individuals presenting with macrophage crown-like structures (CLSs), an indicator of adipose tissue inflammation (*11, 12*), also displayed a decrease in Sfrp5 transcript expression compared with obese individuals that were negative for CLS (fig. S4). CLS-positive individuals also displayed higher levels of adipose TNFα transcript expression and an increase in the homeostasis assessment model for insulin resistance (HOMA-IR) index.

To investigate whether Sfrp5 regulates metabolism, we studied Sfrp5-deficient ($Sfrp5^{-/-}$) mice fed normal or HF-HS diets. No significant differences in body weight (BW) (WT mice: 33.1 T 0.8 g and $Sfrp5^{-/-}$ mice: 34.1 ± 1.1 g), glucose disposal, or insulin sensitivity could be detected between $Sfrp5^{-/-}$ and WT mice when mice were given standard feed (Fig. 2A). However, feeding the HF-HS diet to $Sfrp5^{-/-}$ mice for 12 weeks led to significant impairments in glucose clearance and insulin sensitivity compared with results in WT mice (Fig. 2A). Although $Sfrp5^{-/-}$ mice fed a HF-HS diet showed a small, but significant, increase in BW compared with WT mice, both strains had similar daily food intake during the experimental period of HF-HS diet feeding (fig. S5). Fasting glucose and insulin levels were elevated, and a greater degree of hepatic steatosis, with a higher triglyceride content and heavier liver weight, were observed in $Sfrp5^{-/-}$ mice compared with WT mice fed the HF-HS diet (Fig. 2B and fig. S5). We also performed histological analyses on epididymal adipose tissues. $Sfrp5^{-/-}$ mice fed a HF-HS diet had larger adipocytes than WT mice fed the same diet (Fig. 2C). Thus, Sfrp5-deficiency produces a phenotype of metabolic dysfunction only in mice that are under obesity-induced metabolic stress and not in mice under normal nutritional conditions.

The development of insulin resistance is linked to a macrophage-mediated inflammation of adi-pose tissues (*13–15*). Thus, to determine whether $Sfrp5^{-/-}$ mice show signs of an increased inflammatory response, the macrophage content of adi-pose tissue from $Sfrp5^{-/-}$ and WT mice was measured. Cells positive for F4/80, a macrophage marker, were more abundant in adipose tissue of $Sfrp5^{-/-}$ mice than that of WT mice when both strains were fed a HF-HS diet (Fig. 2D). Consistent with this finding, transcript levels of F4/80 and CD68, another macrophage marker, were significantly elevated in epididymal adipose tissue of $Sfrp5^{-/-}$ mice compared with WT mice fed a HF-HS diet, but not when given normal feed (fig. S6). We also examined the expression levels of proinflammatory mediators in the stromal vascular fractions isolated from epididymal adipose tissue. When mice were fed a

HF-HS diet, significant increases in levels of TNFα, IL-6, and monocyte chemotactic protein–1(MCP-1) transcripts occurred in the stromal vascular fraction from fat tissue of *Sfrp5*$^{-/-}$ mice compared with WT mice (fig. S6). Transcript levels of TNFα, IL-6, and MCP-1 did not differ between *Sfrp5*$^{-/-}$ and WT mice when given normal feed.

To analyze the downstream signaling pathways affected by Sfrp5 deficiency, we assessed whether the canonical or noncanonical Wnt signaling pathways were activated in epididymal adipose tissues of *Sfrp5*$^{-/-}$ and WT mice fed a HF-HS diet. No differences were detected in transcript expression of cyclin D1 or WISP-2, indicators of canonical Wnt signaling, between *Sfrp5*$^{-/-}$ and WT mice (fig. S6). In contrast, phosphorylation of c-Jun N-terminal kinase (JNK), a downstream target of the noncanonical Wnt signaling (*16, 17*), was elevated 2.0 ± 0.1 ($P < 0.05$) in white adipose tissue in *Sfrp5*$^{-/-}$ mice. Also, the phosphorylation of c-Jun, a downstream substrate of JNK, was elevated in *Sfrp5*$^{-/-}$ mice by a factor of 2.3 ± 0.2 ($P < 0.05$) compared with WT mice (Fig. 3A). Activation of JNK1 promotes insulin resistance through serine phosphorylation of insulin receptor substrate–1 (IRS-1) (*18*). We found that IRS-1 phosphorylation at residue Ser^{307} was increased in fat tissue of *Sfrp5*$^{-/-}$ mice by a factor of 2.2 ± 0.3 ($P < 0.05$) compared with WT mice (Fig. 3A). We also assessed insulin signaling in adipose tissue by measuring the activating phosphorylation of Akt at Ser^{473} after systemic insulin administration. In WT mice fed a HF-HS diet, insulin stimulated the phosphorylation of Akt in fat pads, but this induction of phosphorylation was diminished in the HF-HS diet–fed *Sfrp5*$^{-/-}$ mice (Fig. 3B). Because activation of JNK causes obesity-induced insulin resistance (*18*), we hypothesized that the enhanced metabolic dysfunction observed in HF-HS diet–fed *Sfrp5*$^{-/-}$ mice could be attributed to the noncanonical activation of JNK in fat tissues.

To determine the effect of Sfrp5 and Wnt5a on JNK activation at the cellular level, we transduced 3T3-L1 adipocytes with adenoviral vectors encoding Sfrp5 (Ad-Sfrp5) or β-galactosidase (Ad–β-gal) as controls, then incubated the cells with Wnt5a protein. Compared with control vector, Ad-Sfrp5 increased Sfrp5 protein levels in both cell lysates and media (fig. S7) and cancelled the stimulatory effects of Wnt5a on the phosphorylation of JNK in adipocytes (Fig. 3C). Consistent with findings from mice, neither Sfrp5 nor Wnt5a had an effect on TOPflash reporter activity, which transcriptionally responds to canonical Wnt signaling (fig. S7).

To assess the effect of Sfrp5 on JNK activation and inflammatory responses in macrophages in vitro, we stimulated murine macrophages with Wnt5a protein in the presence of conditioned media from 3T3-L1 adipocytes transduced with Ad-Sfrp5 or Ad–β-gal. Wnt5a-stimulated JNK phosphorylation in macrophages was blocked by the conditioned medium from adipocytes transduced with Ad-Sfrp5, but not Ad–β-gal (Fig. 3D). Treatment with Wnt5a also increased TNFα and IL-6 transcript expression by macrophages, and this was also blocked by conditioned medium from Ad-Sfrp5–transduced adipocytes (fig. S8). To explore whether JNK signaling contributes to Wnt5a-stimulated induction of TNFα and IL-6, we pretreated macrophages with the JNK inhibitor SP600125 and incubated the cells with Wnt5a. Pretreatment with SP600125 diminished Wnt5a-stimulated expression of TNFα and IL-6 (fig. S8), which indicated that Sfrp5 blocks macrophage activation through inhibition of Wnt5a-JNK signaling. Similarly, the stimulatory effect of Wnt5a on IL-6 expression in adipocytes was blocked by transduction with Ad-Sfrp5 or pretreatment with SP600125 (fig. S7).

To investigate the role of JNK1 activation in the dysfunctional metabolic phenotype of the Sfrp5-deficient mice, we generated mice lacking both *Sfrp5* and *Jnk1*. Consistent with a previous report (*18*), *Jnk1*$^{-/-}$ mice exhibited improvements in insulin and glucose sensitivity, as well as reduced BW, compared with WT mice when fed the HF-HS diet (Fig. 3E and fig.

S9). Whereas *Sfrp5*$^{-/-}$ mice showed profound insulin resistance and glucose intolerance, *Sfrp5*$^{-/-}$*Jnk1*$^{-/-}$ double-knockout (DKO) mice showed glucose disposal responses that were comparable with those of *Jnk1*$^{-/-}$ mice (Fig. 3E). Furthermore, although BW and transcript levels of TNFα, IL-6, and MCP-1 in fat tissue were elevated in *Sfrp5*$^{-/-}$ mice compared with WT mice, BW and proinflammatory mediator expression levels did not differ for *Jnk1*$^{-/-}$ and *Sfrp5*$^{-/-}$*Jnk1*$^{-/-}$ mice (fig. S9). Thus, the impaired insulin sensitivity and enhanced adipose tissue inflammation in *Sfrp5*$^{-/-}$ mice can be attributed to enhanced activation of JNK1.

To assess whether Sfrp5 can prevent the development of insulin resistance in vivo, we intravenously administered Ad-Sfrp5 or Ad–β-gal to WT and *Sfrp5*$^{-/-}$ mice that were fed a HF-HS diet. Both WT and *Sfrp5*$^{-/-}$ mice treated with Ad-Sfrp5 showed significant improvements in glucose clearance compared with mice treated with the control vector (fig. S10). To investigate the effect of Sfrp5 treatment on glucose metabolism in another model of metabolic dysfunction, we delivered Ad-Sfrp5 or Ad–β-gal into ob/ob mice. Parallel experiments examined the consequences of intravenous injection of an adenoviral vector expressing APN (Ad-APN), because the chronic overexpression of this adipokine has been shown to reverse the metabolic consequences of leptin deficiency (*19*). Two weeks after treatment with Ad-Sfrp5, glucose and insulin sensitivity were significantly improved (Fig. 4A). The administration of Ad-APN to ob/ob mice led to a threefold increase in plasma APN levels, but this was relatively ineffective in improving glucose clearance in this model. The administration of Ad-Sfrp5 also led to significant reductions in transcript levels of TNFα, IL-6, MCP-1, F4/80, and CD68 in adipose tissue, and this was accompanied by a reduction in the activating phosphorylation of JNK (fig. S11). Treatment with Ad-Sfrp5 also led to the atrophy of enlarged white adipocytes in ob/ob mice (Fig. 4B) with a reduction of fat weight (Ad–β-gal: 2.51 ± 0.19 g and Ad-Sfrp5: 2.01 ± 0.11 g, $P < 0.05$) and a marked attenuation of lipid accumulation in the liver (Fig. 4C). Taken together, these data indicate that acute Sfrp5 administration can reverse hyperglycemia and hepatic steatosis in multiple mouse models of metabolic dysfunction.

In summary, we show that Sfrp5 is secreted by adipocytes and that it controls the micro-environment of white adipose tissue under conditions of metabolic stress. Whereas Sfrp5$^{-/-}$ mice do not express a detectable phenotype when given normal feed, these animals displayed aggravated fat pad inflammation and systemic metabolic dysfunction when fed a high-calorie diet. Conversely, the acute administration of Sfrp5 to models of obese and diabetic mice improved metabolic function and reduced adipose tissue inflammation. We propose that Sfrp5 neutralizes noncanonical JNK activation by Wnt5a in macrophages and adipocytes via paracrine and autocrine mechanisms, respectively. The JNK signaling pathway in adipocytes and macrophages has emerged as an important mediator of adipose tissue inflammation that affects systemic metabolism (*18, 20–22*). Thus, the Sfrp5-JNK1 regulatory axis in fat represents a potential target for the control of obesity-linked abnormalities in glucose homeostasis.

Supplementary Material

Refer to Web version on PubMed Central for supplementary material.

References and Notes

1. Spiegelman BM, Flier JS. Cell. 1996; 87:377. [PubMed: 8898192]
2. Ouchi N, Kihara S, Funahashi T, Matsuzawa Y, Walsh K. Curr. Opin. Lipidol. 2003; 14:561. [PubMed: 14624132]
3. Scherer PE. Diabetes. 2006; 55:1537. [PubMed: 16731815]

4. Shibata R, et al. Nat. Med. 2005; 11:1096. [PubMed: 16155579]
5. Izumiya Y, et al. Cell Metab. 2008; 7:159. [PubMed: 18249175]
6. Materials and methods are available as supporting material on *Science* Online.
7. Bovolenta P, Esteve P, Ruiz JM, Cisneros E, Lopez-Rios J. J. Cell Sci. 2008; 121:737. [PubMed: 18322270]
8. Kawano Y, Kypta R. J. Cell Sci. 2003; 116:2627. [PubMed: 12775774]
9. Ross SE, et al. Science. 2000; 289:950. [PubMed: 10937998]
10. Li Y, et al. Genes Dev. 2008; 22:3050. [PubMed: 18981481]
11. Apovian CM, et al. Arterioscler. Thromb. Vasc. Biol. 2008; 28:1654. [PubMed: 18566296]
12. Cinti S, et al. J. Lipid Res. 2005; 46:2347. [PubMed: 16150820]
13. Hotamisligil GS. Nature. 2006; 444:860. [PubMed: 17167474]
14. Weisberg SP, et al. J. Clin. Invest. 2003; 112:1796. [PubMed: 14679176]
15. Xu H, et al. J. Clin. Invest. 2003; 112:1821. [PubMed: 14679177]
16. Veeman MT, Axelrod JD, Moon RT. Dev. Cell. 2003; 5:367. [PubMed: 12967557]
17. Yamanaka H, et al. EMBO Rep. 2002; 3:69. [PubMed: 11751577]
18. Hirosumi J, et al. Nature. 2002; 420:333. [PubMed: 12447443]
19. Kim JY, et al. J. Clin. Invest. 2007; 117:2621. [PubMed: 17717599]
20. Solinas G, et al. Cell Metab. 2007; 6:386. [PubMed: 17983584]
21. Sabio G, et al. Science. 2008; 322:1539. [PubMed: 19056984]
22. Vallerie SN, Furuhashi M, Fucho R, Hotamisligil GS, Maedler K. PLoS ONE. 2008; 3:e3151. [PubMed: 18773087]
23. We thank S. Sono-Romanelli for technical assistance. Funded by National Institutes of Health grants (AG34972, HL86785, AG15052, and HL81587) to K.W.

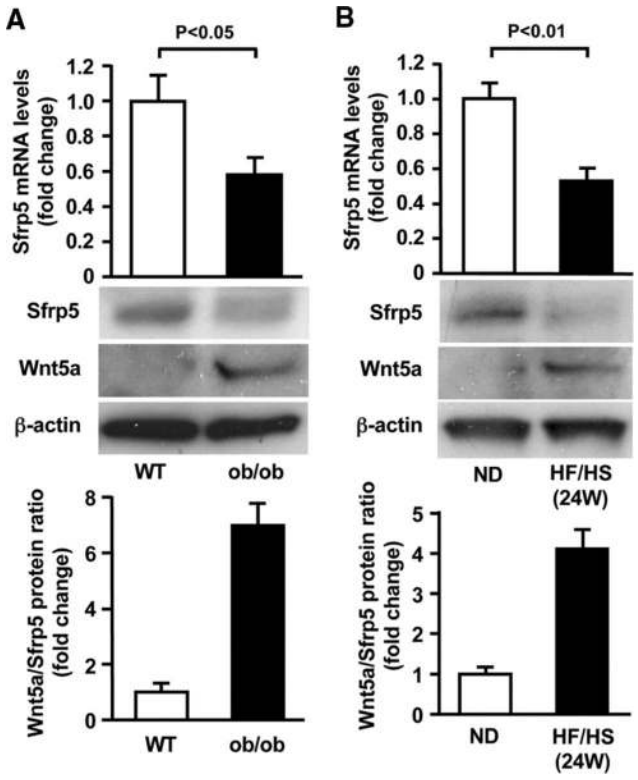

Fig. 1.

Expression of Sfrp5 in white adipose tissue in lean and obese mice. (**A**) Expression of Sfrp5 and Wnt5a in epididymal fat tissue in WT and ob/ob mice at the age of 20 weeks. (**B**) Expression of Sfrp5 and Wnt5a in epididymal adipose tissue of WT mice fed normal diet (ND) or HF-HS diet for 24 weeks. Sfrp5 transcript levels were measured by quantitative real-time polymerase chain reaction analysis and expressed relative to a reference gene, 36B4 (n = 6 or 7 mice). Expression of Sfrp5 and Wnt5a protein was determined by immunoblot analysis.

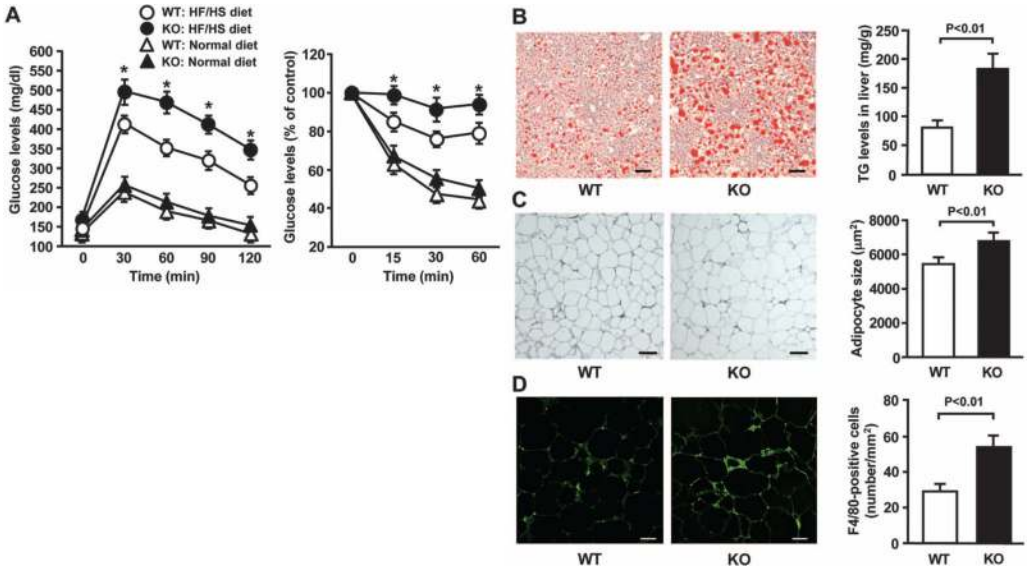

Fig. 2.

Sfrp5-deficiency exacerbates metabolic dysfunction in mice fed a HFHS diet. *Sfrp5*$^{-/-}$ (KO) and WT mice were given normal feed or a HF-HS diet for 12 weeks. (**A**) (Left) Glucose tolerance and (right) insulin tolerance tests ($n = 9$ in each group). *$P < 0.01$ versus corresponding WT mice. (**B**) Histological sections of oil red O–stained liver from the HF-HS–fed WT and KO mice. Scale bars, 100 μm. (Right) Triglyceride (TG) content of liver from HF-HS diet–fed WT and KO mice ($n = 6$). (**C**) Histological analysis of hematoxylin and eosin (H&E)–stained epididymal white adipose tissue of the HF-HS–fed WT and KO mice. Scale bars, 100 μm. Adipocyte cross-sectional areas were determined using the ImageJ program ($n = 7$). (**D**) Macrophage accumulation in epididymal adipose tissues in WT and KO mice when fed a HF-HS diet. Histological sections were stained with antibody against F4/80. Macrophage infiltration was determined as the number of F4/80-positive cells per mm^2 ($n = 8$). Scale bars, 50 μm.

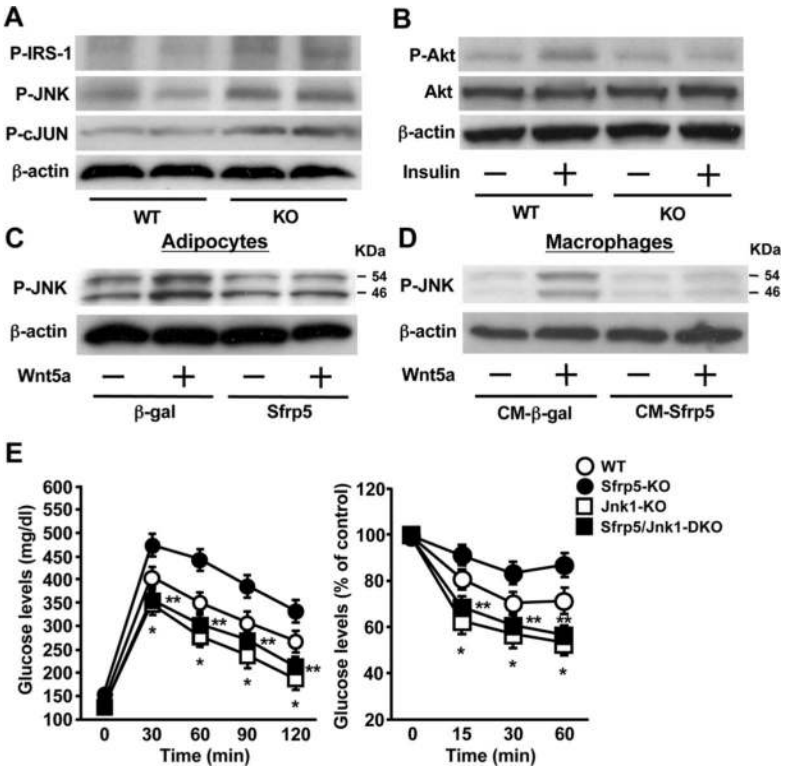

Fig. 3.

JNK1 activation contributes to diet-induced metabolic dysfunction in Sfrp5-deficient mice and Wnt5a-mediated cell activation in vitro. *Sfrp5*$^{-/-}$ (KO) and WT mice were maintained on a HF-HS diet for 12 weeks. (**A**) Phosphorylation of JNK (Thr^{183}/Tyr^{185}), cJUN (Ser^{63}), and IRS-1 (Ser^{307}) in fat tissue of WT and KO mice as determined by immunoblot analysis. (**B**) Akt phosphorylation in adipose tissues of WT and KO mice after insulin administration. (**C**) Effect of Sfrp5 on Wnt5a-stimulated JNK phosphorylation in adipocytes. 3T3-L1 adipocytes were transduced with Ad–β-gal or Ad-Sfrp5 in the presence of AdCMV-tTA, which uses a cytomegalovirus promoter sequence to drive a tetracycline transactivator and activate β-galactosidase or Sfrp5, followed by treatment with Wnt5a or vehicle for 30 min. (**D**) Effect of the conditioned medium from Sfrp5-transfected adipocytes on Wnt5a-induced JNK activation in macrophages. Peritoneal macrophages were stimulated with Wnt5a or vehicle for 30 min in the presence of the conditioned media from 3T3-L1 adipocyte transduced with Ad–β-gal or Ad-Sfrp5 along with AdCMV-tTA. (**E**) Contribution of JNK1 to severe insulin resistance caused by Sfrp5 deficiency. WT, *Sfrp5*$^{-/-}$ (Sfrp5-KO), *Jnk1*$^{-/-}$ (Jnk1-KO), and *Sfrp5*$^{-/-}$ *Jnk1*$^{-/-}$ (Sfrp5/Jnk1-DKO) mice were maintained on a HF-HS diet for 12 weeks. (Left) Glucose tolerance and (right) insulin tolerance tests were performed (n = 6 or 7 in each group). *P < 0.01 versus WT mice. **P < 0.01 versus Sfrp5-KO mice.

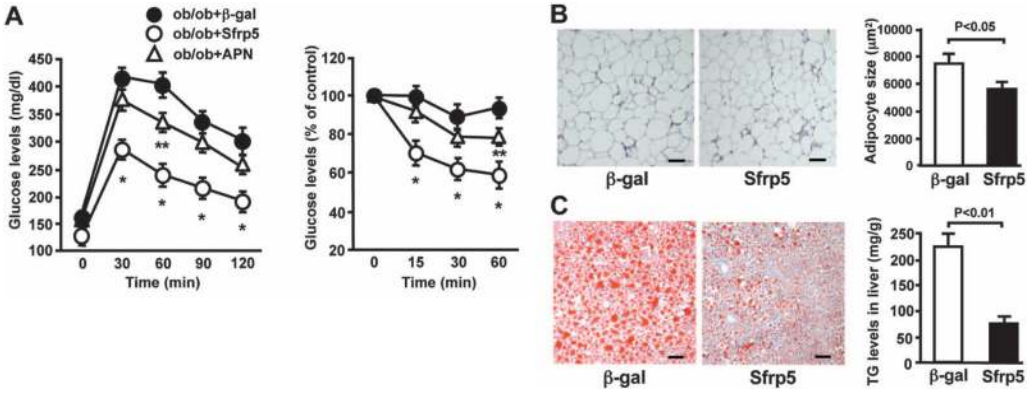

Fig. 4.

Systemic delivery of Sfrp5 is protective against metabolic dysfunction in obese mice. (**A**) (Left) Glucose tolerance and (right) insulin tolerance assays. Ad–β-gal and Ad-Sfrp5 along with AdCMV-tTA, or Ad-APN were intravenously administered to ob/ob mice at the age of 20 weeks. Two weeks after supplementation of adenoviral reagents (β-gal, Sfrp5, or APN), glucose tolerance and insulin tolerance tests were performed ($n = 5$ or 6 in each group). *$P <$ 0.01 versus β-gal treatment. **$P < 0.05$ versus β-gal treatment. (**B** and **C**) Representative histological sections of (B) fat pads stained with H&E and (C) liver stained with oil red O in β-gal– or Sfrp5-treated ob/ob mice. Scale bars, 100 μm. (B) (Right) Quantification of adipocyte size ($n = 6$). (C) (Right) Triglyceride (TG) content of liver ($n = 6$).